

# Chemo-kinematic analysis of metal-poor stars with unsupervised machine learning

André R. da Silva<sup>1</sup>, Rodolfo Smiljanic<sup>1</sup>, and Riano E. Giribaldi<sup>1</sup>

<sup>1</sup>*Nicolaus Copernicus Astronomical Center, Polish Academy of Sciences, ul. Bartycka 18, 00-716, Warsaw, Poland; arodrigo@camk.edu.pl*

## Abstract.

Metal-poor stars play an important role in the understanding of Galaxy formation and evolution. Evidence of the early mergers that built up the Galaxy might remain in the distributions of abundances, kinematics, and orbital parameters of the stars. In this work, we report on preliminary results of an on-going chemo-kinematic analysis of a sample of metal-poor ( $[\text{Fe}/\text{H}] \leq -1.0$ ) stars observed by the GALAH spectroscopic survey. We explored the chemical and orbital data with unsupervised machine learning (hierarchical clustering, k-means cluster analysis and correlation matrices). Our final goal is to find an optimal way to separate different Galactic stellar populations and stellar groups originating from merging events, such as Gaia-Enceladus and Sequoia.

## 1. Introduction

Galaxies grow through the accretion and merging of smaller stellar systems (e.g., Bland-Hawthorn & Freeman 2014). It is sometimes possible to identify signatures of these early mergers as chemo-kinematic stellar substructures. In many instances, however, the criteria used to separate and study such substructures is arbitrarily defined by carving boxes out of the parameter space. In this work, we are investigating ways to improve the selection criteria using unsupervised machine learning, and trying to account for the possible distributions of stellar properties of the objects belonging to each substructure.

The first unequivocal evidence of mergers was the discovery of the Sagittarius dwarf galaxy by Ibata et al. (1994). Since then, others have discovered more pieces of the Galactic merger puzzle. Recently, Helmi et al. (2018) and Belokurov et al. (2018) independently discovered a possible merger that occurred in the Milky Way about 8-11 Gyr ago. The object that merged with the Galaxy, often called Gaia-Enceladus or Gaia-Sausage (GES), could be the origin of the inner halo and the thick disk of the Milky Way (Helmi et al. 2018). The second data release (DR2) of *Gaia* (Gaia Collaboration 2018) has helped in the identification of additional merger candidates such as the Sequoia (Myeong et al. 2018) and the Thamnos substructures (Koppelman et al. 2019).

## 2. Data and analysis

In this work, we used the proper motions and parallaxes of *Gaia* DR2. Chemical parameters were obtained from the DR2 of GALAH (Galactic Archaeology with Hermes, Buder et al. 2018). GALAH delivered chemical abundances of 26 chemical el-

ements for  $\sim 340\,000$  stars from the analysis of spectra with  $R \sim 28\,000$ . We cross-matched metal-poor stars from the GALAH survey (selected with  $[\text{Fe}/\text{H}] \leq -1.0$ ,  $2.0 \leq \log g \leq 5.0$ ,  $T_{\text{eff}} \geq 4\text{ kK}$  and with `cannon_flag = 0`) with *Gaia* (selecting those with  $\sigma_{\varpi}/\varpi < 20\%$ ). This resulted in 1 072 stars.

Using *Gaia* proper motions and GALAH radial velocities, we then integrated the stellar orbits using *galpy* (Bovy 2015) for a period of 10 Gyr using the Milky Way potential from McMillan (2017). From *galpy*, we extracted the action angles ( $J_r, J_\phi, J_z$ ), two integrals of motion ( $E, L_z$ ), eccentricity, cylindrical radius, and other orbital parameters. We also performed Monte Carlo simulations in order to estimate the uncertainties.

t-distributed stochastic neighbor embedding (t-SNE) is a manifold learning method that uses affinity between the data points as probability. This is particularly useful for exploring structures from an  $N$  dimensional problem in a 2D map. The location of the points in this map is given by minimizing the Kullback-Leibler divergence. For the analysis that we report here, we used t-SNE to identify the stars in our sample that are close together in the parameter space. The quantities used were:  $J_r, J_\phi, J_z$ , and the orbital eccentricity, together with the chemical parameters  $[\text{Fe}/\text{H}]$  - representing iron-peak elements,  $[\text{Mg}/\text{Fe}]$  - representing the  $\alpha$ -elements,  $[\text{Ba}/\text{Fe}]$  - representing the s-process elements and  $[\text{Eu}/\text{Fe}]$  - representing the r-process elements.

In order to decide which is the best number of cluster components for these data, we did a k-means clustering analysis with increasing number of clusters. The first number of clusters past the mark of 95% of distortion explanation was considered as the optimal number (in this case nine). We then used agglomerative clustering using Ward hierarchical method to separate the t-SNE map into the nine clusters. We used the python module scikit-learn (Pedregosa et al. 2011) to perform this analysis.

### 3. Discussion

In Fig. 1, the t-SNE map is shown with the color-coded clusters. The definition of structures associated to mergers have in general been done using only kinematical parameters (see Helmi et al. 2018; Belokurov et al. 2018; Myeong et al. 2018; Massari et al. 2019), with a few exceptions like in Naidu et al. (2020). Massari et al. (2019) and Myeong et al. (2018) disagree on criteria used to classify the GES and Sequoia stars (see Fig. 2). Figure 3 helps to compare which proposed Galactic substructures found in the literature is closer to each of the clusters that we found.

Comparing the results of our analysis with those of the literature, we find that: in gray scale, we have the stellar groups that correspond to what is generally agreed to be the disk of the Galaxy; in pink scale is the GES close to the limits defined by Massari et al. (2019); the red points agree with Myeong et al. (2018) and Naidu et al. (2020) for the Sequoia substructure; the stars in blue are intermediary between the disk and the halo of the Milky Way; and the lighter blue cluster is on the same region as Naidu et al. (2020) defines the Wukong substructure (as a prograde, metal-poor and  $\alpha$ -rich substructure). In Fig. 4, it is possible to separate the pink shaded group from the gray. The dark blue cluster is on the same region of what Naidu et al. (2020) called a “metal-weak thick disk”. To summarize, we found that unsupervised machine learning techniques are powerful tools that can help to recover halo substructures associated to early merging events of the Milky Way.

**Acknowledgments.** A.R.S, R.S., and R.E.G. acknowledge support by the Polish National Science Centre through project 2018/31/B/ST9/01469.

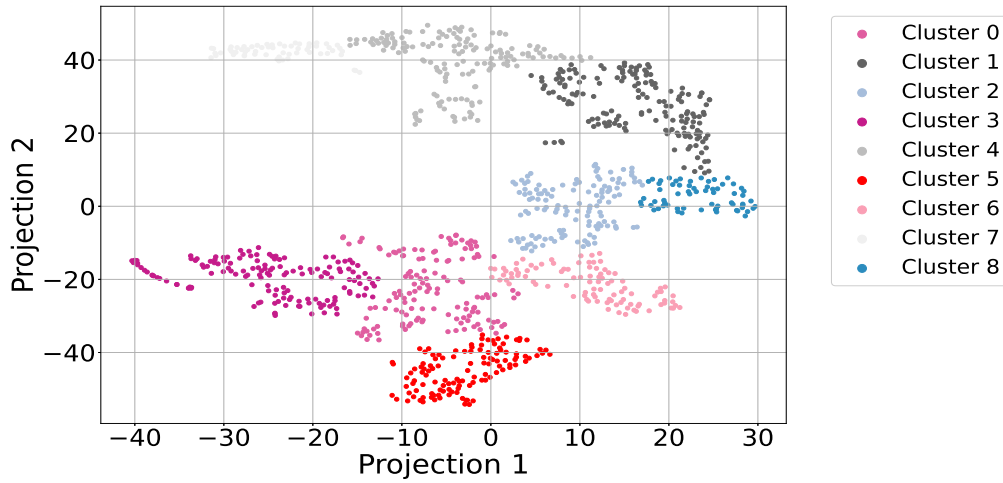


Figure 1. t-SNE projection of the parameter space for  $J_\phi$ ,  $J_r$ ,  $J_z$ ,  $[\text{Fe}/\text{H}]$ ,  $[\text{Mg}/\text{Fe}]$ ,  $[\text{Ba}/\text{Fe}]$ ,  $[\text{Eu}/\text{Fe}]$ , orbital eccentricity. Gray-colored symbols represent the disk, in pink is the Gaia-Enceladus-Sausage (GES), in red is Sequoia and in blue the thick disk transition to the halo.

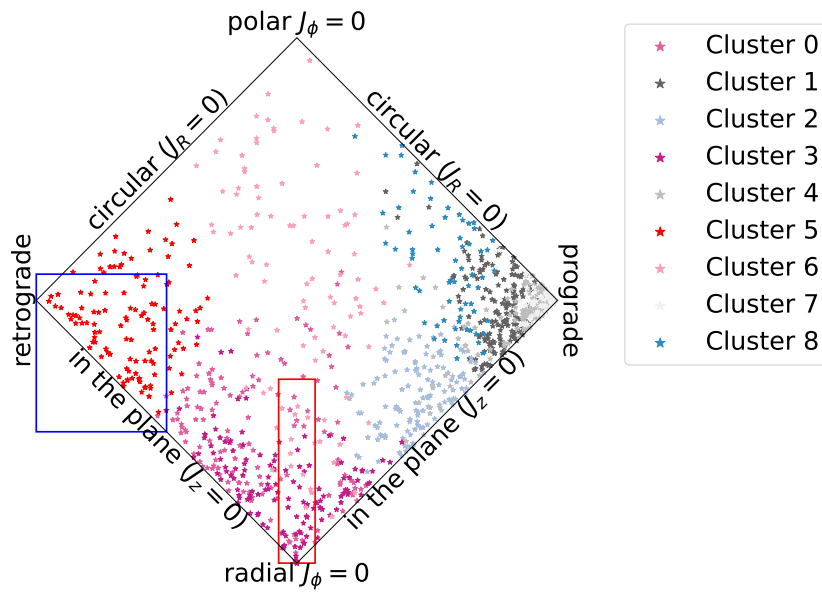


Figure 2. Action angles by total action. The blue box represents the limits of Sequoia in Myeong et al. (2018) and the red box the limits of GES in Myeong et al. (2018). Cluster 5 (in red) agrees with Myeong et al. (2018).

## References

- Belokurov, V., Erkal, D., Evans, N. W., Koposov, S. E., & Deason, A. J. 2018, *MNRAS*, 478, 611
- Bland-Hawthorn, J., & Freeman, K. 2014, *Saas-Fee Advanced Course*, 37, 1
- Bovy, J. 2015, *ApJS*, 216, 29

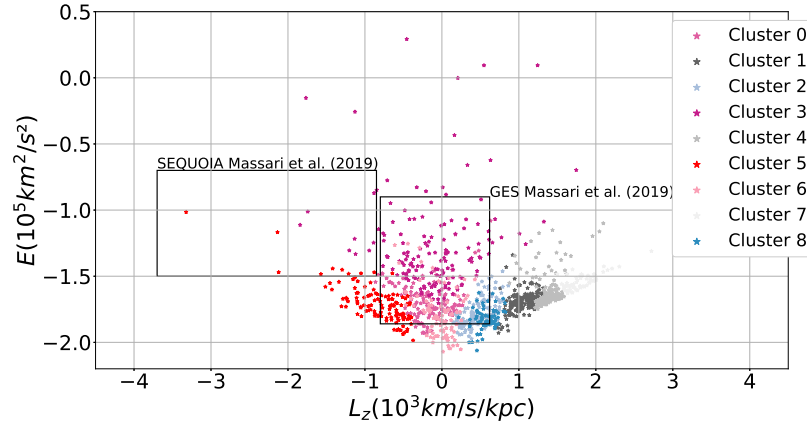


Figure 3. Total orbital energy by angular momentum in the Galactic pole direction (Lindblad diagram). Points colored in intermediate pink could be Wukong as described by Naidu et al. (2020).

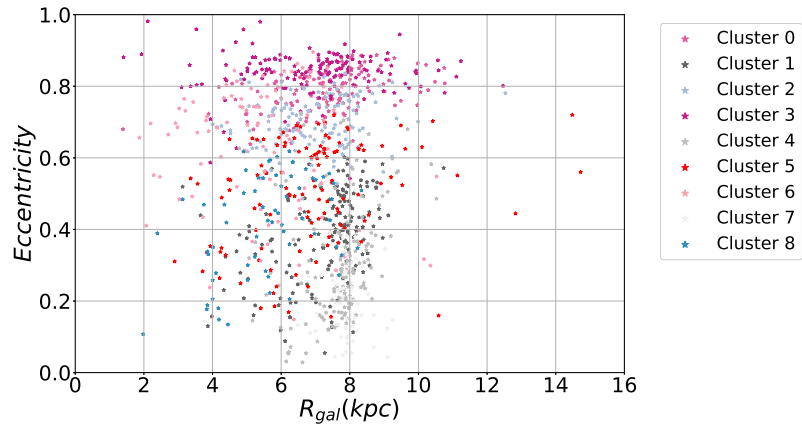


Figure 4. Orbital eccentricity by the average cylindrical radius of the orbit. The GES stars are mostly concentrated in high eccentricity.

- Buder, S., Asplund, M., Duong, L., & Galah Collaboration 2018, MNRAS, 478, 4513  
 Gaia Collaboration 2018, A&A, 616, A1  
 Helmi, A., Babusiaux, C., Koppelman, H. H., Massari, D., Veljanoski, J., & Brown, A. G. A. 2018, Nat, 563, 85  
 Ibata, R. A., Gilmore, G., & Irwin, M. J. 1994, Nat, 370, 194  
 Koppelman, H. H., Helmi, A., Massari, D., Price-Whelan, A. M., & Starkenburg, T. K. 2019, A&A, 631, L9  
 Massari, D., Koppelman, H. H., & Helmi, A. 2019, A&A, 630, L4  
 McMillan, P. J. 2017, MNRAS, 465, 76  
 Myeong, G. C., Evans, N. W., Belokurov, V., Sanders, J. L., & Koposov, S. E. 2018, ApJ, 863, L28  
 Naidu, R. P., Conroy, C., Bonaca, A., Johnson, B. D., Ting, Y.-S., Caldwell, N., Zaritsky, D., & Cargile, P. A. 2020, ApJ, 901, 48  
 Pedregosa, F., Varoquaux, G., Gramfort, A., Michel, V., Thirion, B., Grisel, O., Blondel, M., Prettenhofer, P., Weiss, R., Dubourg, V., et al. 2011, the Journal of machine Learning research, 12, 2825